DISASTER SCIENCE AND ENGINEERING p. 31-37, 1(2), 2015

Source Mechanism And Stress Changes Of The January 25, 2005 Hakkari (Eastern Turkey) Earthquake (Mw=5.7) : Implications For The Earthquake Hazard

Murat Utkucu[1], Kubilay Atalay[2], Emrah Budakoğlu[3] , Çetin Yeşilova[4]

Received: 17.12.2015 Accepted: 29.12.2015

Abstract: The source mechanism of the January 25, 2005 Hakkari earthquake is obtained from both *P* wave first motion polarities and waveform modeling. The source mechanism derived from the *P* wave motion polarities has indicated a dextral faulting along a NW-SE trending rupture plane while sinistral faulting along a NE_SW trending rupture plane. A point-source waveform inversion technique is applied to the teleseismically recorded *P* and *SH* waveforms of the earthquake to derive the source process. The data has been satisfactorily matched using two-subevent source process indicating a complex source process with a relatively large strike-slip faulting subevent that followed by a smaller oblique normal faulting subevent. The fact that the active fault map indicate a NW-SE trending thrust fault and NE-SW trending sinistral Akçalı fault in the near source region has prompted us to select the NE-SW trending nodal planes from both solutions as the fault plane. It is suggested that the earthquake was produced by the Akçalı fault and the faulting is left-lateral. The overall source process implies a predominantly left-lateral faulting (strike=201°, dip=69°, rake=-24°) with a seismic moment of 3.5×10^{17} Nm ($M_W \approx 5.7$). A stress changes due to rupture along the Akçalı fault well explained the $M \geq 4$ seismicity after the earthquake, thus supporting a NE-SW striking fault. The Yüksekova-Şemdinli Fault Zone, which produced most of the following seismicity, was considerably stressed. The results further suggest active strike-slip faulting within or in the very neighborhood of the Bitlis Thrust Zone.

***Index Terms*—** The 25 January 2005 Hakkari earthquake, eastern Turkey, Bitlis thrust Zone, teleseismic point-source analysis

I. INTRODUCTION

The 25 January 2005 Hakkari earthquake (M_W=5.7) occurred on the south boundary of the eastern Anatolian block known as Bitlis Thrust Zone (BTZ) (Figs. 1 ve 2). Arabian and Anatolian plates collide along the BTZ [1, 2]. Recent studies have shown that the deformation related to the northward movement of the Arabian plate is mainly transferred to the Caucasian thrust zone lying in the NE via distributed strike-slip faults within the eastern Anatolian block [3, 4, 5, 6] (Fig. 2). Right-lateral Yüksekova-Şemdinli and left-lateral Başkale, Arındı and Akçalı faults are the member of these strike-slip faults lying close to the epicenter of the 2005 Hakkari earthquake [7, 8]. These tectonic features have caused an intense seismic activity in the near source region both in instrumental [9, 10] and historical [11, 12] periods (Figs. 2 and 3).

The 25 January 2005 Hakkari earthquake (M_W 5.7) occurred on the BTZ (Figs. 1 and 2), [7, 9, 13]. The earthquake was strongly felt in the Van-Hakkari area, leading to 2 deaths and 26 injured peoples. Hypocentral and source parameters of the earthquake estimated by different seismological institutes and studies are summarized in Table 1. The source mechanism solutions suggest that the earthquake was due to strike-slip faulting.

In the present study, the source parameters of the 25 January 2005 Hakkari earthquake have been obtained from both *P* wave first motion polarities and teleseismic point-source analysis [14]. Then Coulomb static stress changes caused by the earthquake have been calculated and overall results utilized to discuss importance of strike slip faulting earthquake hazard of the source region.

[1]Sakarya University, Department of Geophysics, Sakarya, Turkey
[2]Karadeniz Technical University, Trabzon, Turkey.
[3]Sakarya University, Department of Geophysics, Sakarya, Turkey
[4]Yüzüncü Yıl University, Department of Geology, Van, Turkey

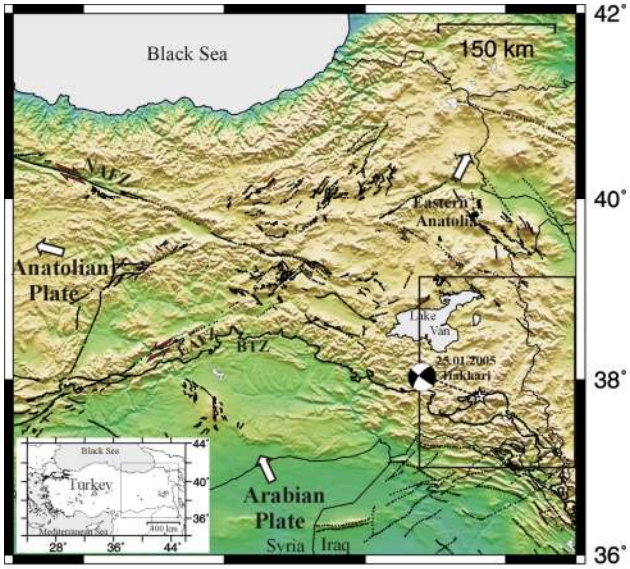

Fig. 1. Major tectonic elements of Eastern Anatolia and epicenter (white star) and the source mechanism of the 25 January 2005 Hakkari earthquake. Extents of faults and relative plate motions are from MTA [6] and Reilinger et al. [8] respectively. Large rectangle encloses the map areas shown in Figs. 2, and 3 and large arrows indicate relative plate motions *NAFZ* North Anatolian Fault Zone, *EAFZ* East Anatolian Fault Zone, *BTZ* Bitlis Thrust Zone

.

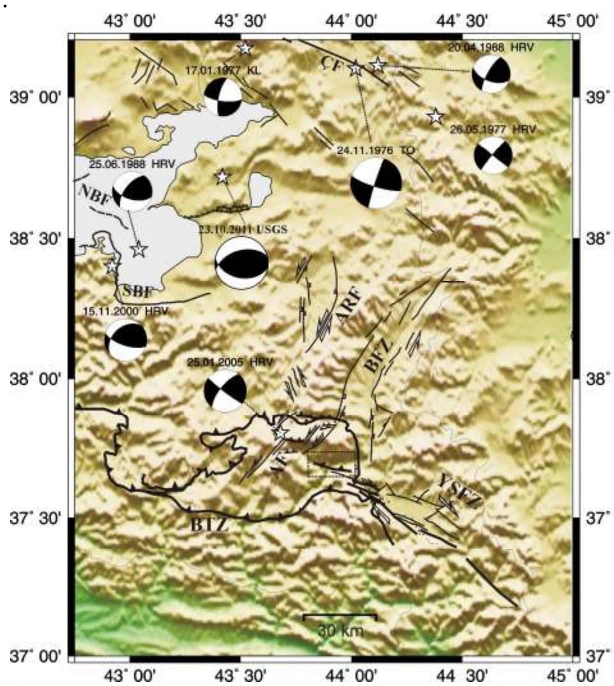

Fig. 2. Local tectonic features and epicentral distribution of large earthquakes (white stars) with available focal mechanisms for Van-Hakkari area. Extents of faults are from Koçyiğit [7] and MTA[8]. The fault within the dashed-lined rectangle was mapped as strike-slip fault by Emre et al. [15] but as a thrust fault in MTA [18]. HRV: Harvard GCMT, TO: Toksöz et al. [16], KL: Kalafat [17]. BTZ: Bitlis Thrust Zone, ÇF: Çaldıran Fault, BFZ: Başkale Fault Zone, YŞFZ: Yüksekova-Şemdinli Fault Zone, AFZ: Arındı Fault Zone, AF: Akçalı Fault, NBF: Northern Boundary Fault, SBF: Southern Northern Boundary Fault.

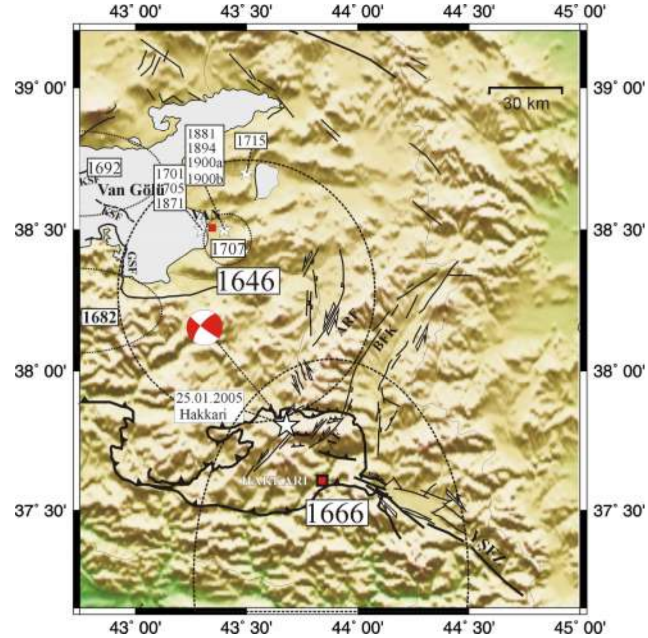

Fig. 3. Historical seismicity of the Van-Hakkari area. The historical earthquakes are compiled from Ambraseys and Finkel [11] Ambraseys [12] Ergin et al. [18]. See caption of Figure 2 for the active fault references.

II. DATA AND METHOD

P wave first motion polarity readings have been taken from International Seismological Centre (ISC) bulletin [19]. The dilatational and compressional readings are manually separated as much as possible by means of trial and error [20].

We have used broadband teleseismic *P* and *SH* velocity waveforms recorded by the IRIS Data Management Centre. The data recorded at teleseismic distances between 30^{o} and 90^{o} have been selected for the analysis in order to avoid upper mantle distortions and core-mantle boundary diffractions. The data are corrected for the instrument responses and bandpass filtered with corner frequencies at 0.01 to 0.33 Hz regarding low signal/noise ratio, especially for the *P* waves. Considering the size of the earthquake a record length of 25 s is chosen for the inversion. A visual check of the waveforms has shown that the selected wave length contains the main source related wave arrivals at each station. *P* waveforms at 7 stations and *SH* waveforms at 9 stations are included in the analysis of the 2005 Hakkari earthquake.

Table 1. Source parameters of the 25 January 2005 Hakkari earthquake.

	Lat. N (°)	Lon. E (°)	Depth (km)	Strike (°)	Dip (°)	Rake (°)	*Mo* (x10^{18} Nm)	Magnitude	
KOERI	37.75	43.79	16					M_D5.5	
USGS[1]	37.62	43.70	41	219	70	-12	0.62	M_W 5.8	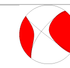
GCMT	37.72	43.72	13.2	209	79	-12	0.75	M_W 5.9	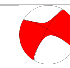
ZUR_RMT	37.62	43.70	24	34	85	2	1.29	*M*w 6.0	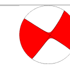
Şengül et al. [13]	37.75	43.79	6	35	68	33		*M*w 5.4	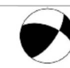
This study				201	69	-24	0.35	*M*w 5.7	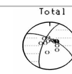

KOERI = Kandilli Observatory and Earthquake Research Institute; USGS[1] = United States Geological Survey body-wave moment tensor solution; GCMT = Global Centroid Moment Tensor Catalogue; ZUR_RMT = Zurich Moment Tensors.

A teleseismic point-source inversion analysis developed by Kikuchi ve Kanamori [14] is used. The method first requires a point-source grid with an assigned strike to represent faulting. The point-source grid defined for the 2005 Hakkari earthquake has 6 and 5 point-sources along strike and depth, respectively, having 3 km separations (Fig. 4). The strike of the grid is initially assigned as 300°, which is approximate strike of the YŞFZ. Third point-source both along the strike and the depth is selected as the reference point. So, the reference point has a depth of 9 km and corresponds to the focus of the earthquake or the rupture initiation point. The rupture velocity is assigned as 2.5 km/sec. We use a trapezoid source-time function that has 5 s total duration and equal rise and fall of 2 s. The crustal velocity structure used for the estimation of synthetic seismograms is adapted from the *P* wave velocity model of Zor et al. [21] (Table 2). Shear-wave velocities *(Vs)* are computed from the *P* wave velocity *(Vp)* by assuming Poisson materials: $Vp = 1.73Vs$. The *SH* waveforms are given larger weights in the inversion due to the low signal/noise ratios of the *P* waveforms.

Coulomb failure stress change ($\Delta\sigma_f$) can be simply expressed as

$$\Delta\sigma_f = \Delta\tau + \mu' \, \Delta\sigma_n \qquad (1)$$

Where $\Delta\tau$ and $\Delta\sigma_n$ represent the changes in the shear and the normal stresses over the fault plane, respectively, while μ' is the apparent coefficient of the friction [22, 23], which includes the unknown effect of pore fluid pressure and has been pointed out to vary in the range 0.2-0.8 [23] and to be not crucial in affecting the pattern of change in Coulomb failure stress [24]. We have used μ'=0.4 in our stress calculations and base them on the coseismic elastic dislocation modelling of the earthquakes [25] by assuming earthquake ruptures as rectangular dislocation surfaces in an elastic half-space having Young's modulus of 8x10^5 bar and Poisson's ratio of 0.25. Fault lengths and slip values are determined from the empirical relations of Wells and Coppersmith (1994). The earthquake rupture represented by a fault plane of 10 km x 6 km with homogeneous slip of 0.25 m.

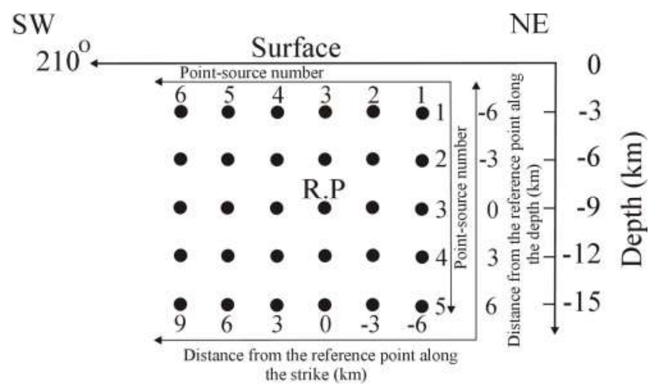

Fig. 4. Point-source grid used for the teleseismic analysis of the 25 January 2005 Hakkari earthquake. RP stands for the reference point.

Table 2. The crustal velocity structure used fort he calculation of the synthetic seismograms in the study (adapted from Zor et. al. [21]).

Depth (km)	Vp (km/s)	Vs (km/s)	Density (ρ) x10^3 kg/m^3
4.0	5.20	3.10	2.60
18.0	6.20	3.60	2.70
28.0	5.20	3.10	3.30
7.0	5.75	3.35	2.60
46.0	6.90	4.00	2.70

III. Results

Many trials have been implemented to find a solution that separates the dilatational and compressional P wave first motion readings as much as possible. Figure 5 reflects the best achieved from the data in the study.

Table 3. The source parameters of the 25 January 2005 Hakkari earthquake resulted from the inversion runs carried out in the study.

Inversion Run	Subevent	Rupture time(s)	Distance (km)	Depth (km)	M_O ($x10^{18}$ Nm)	Strike (°)	Dip (°)	Rake (°)	RMS error
Single point-source modeling (point-source grid strikes 300°)									
IR1	1	1-9	0.0	3.0	0.35	198	87	13	0.458
Double point-source modeling (point-source grid strikes 300°)									
IR2	1	1-8	0.0	3.0	0.38	197	89	-11	0.377
	2	5,5-11	-6.0	-3.0	0.16	241	57	-53	
	Total				0.36	201	71	-21	
Double point-source modeling (point-source grid strikes 210°)									
IR3	1	1-9	0.0	3.0	0.32	197	88	-12	0.374
	2	6-13	-3.0	-3.0	0.15	237	54	-55	
	Total				0.35	201	69	-24	

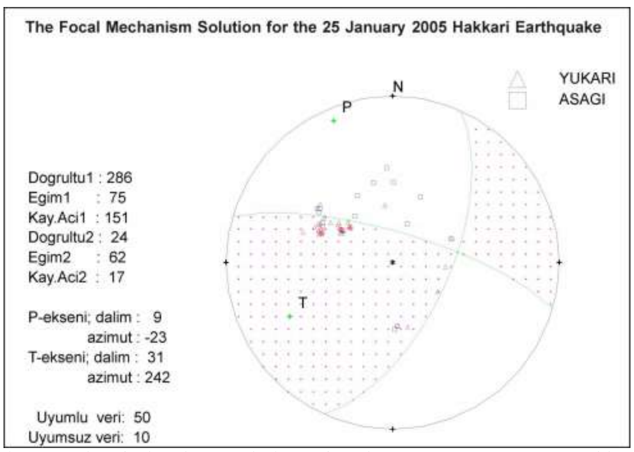

Fig. 5. The fault plane solutions for the 25 January 2005 Hakkari earthquake obtained from the *P* wave first motion polarity readings in ISC Bulletin. The squares and triangles denote dilatational and compressional *P* wave first motion readings, respectively.

The data has been inverted using both single and double subevent source models. These inversion runs are called as "inversion run 1" (IR1) and IR2, respectively. The source parameters for these inversion runs are juxtaposed in Table 3. Both RMS (Root mean squares) errors and visual comparison of the synthetic-observed waveforms suggest that the data could be satisfactorily modeled using double-subevent source model. Another inversion trial (IR3) with double-subevent is also implemented using a point-source grid striking 210 (assumption that the earthquake occurred along the sinistral Akçalı fault) (Fig. 2). This trial has resulted in almost the same RMS error and the rupture process model (Table 3) as the IR2 that corresponds to a faulting along the YŞFZ. This finding suggests that the data do not have the resolution to discriminate between the NE-SW trending sinistral and the NW-SE trending dextral faultings. For visual purposes, the source mechanisms, synthetic-observed waveform comparison and rupture process model for the IR3 have been shown in Fig. 6.

Stress changes caused by the 2005 Hakkari earthquake are resolved both on optimally oriented strike-slip and thrust faults (Fig. 7). The stress patterns in Fig. 7 have been imaged at a depth of 5 km and increase and decrease in the stresses are represented with red and blue colors, respectively. In Fig.7 we also show the $M \geq 4$ seismicity following the earthquake for comparison with the stress changes. The $M \geq 4$ seismicity data obtained from the catalogue of Kandilli Observatory and Earthquake Research Institute.

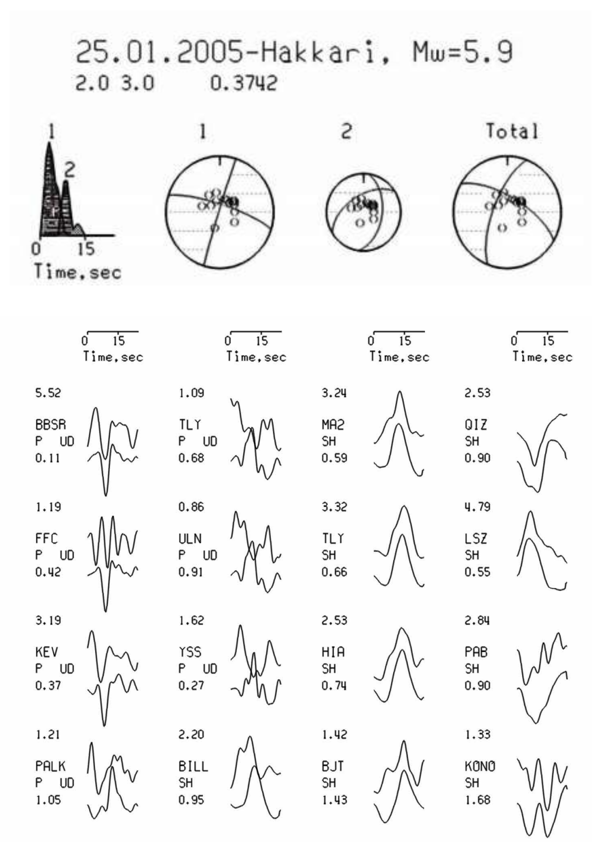

Fig 6. Teleseismic point-source analysis results for the 25 January 2005 Hakkari earthquake obtained from the inversion run IR3. Source time functions, the mechanisms of the subevents and the total mechanism are given at the top while the observed (up) and calculated (down) waveforms are compared at the bottom. The numbers shown to the left of the waveform couples are peak-to-peak amplitudes in microns (up) and the amplitude ratio of calculated to observed seismograms (down).

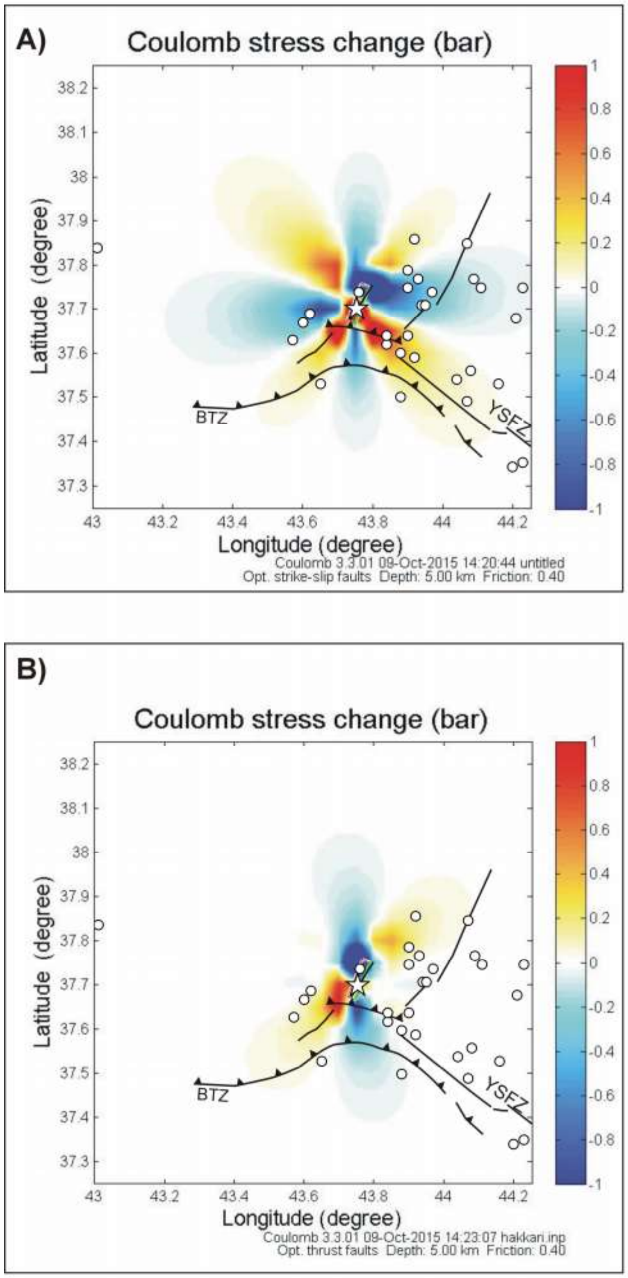

Fig. 7. Maps of Coulomb stress changes caused by the 25 January 2005 Hakkari earthquake calculated over the optimally oriented (a) strike-slip and (b) thrust faults along with the $M \geq 4.0$ seismicity (white circles). Stars denote the epicenter of the 2005 Hakkari earthquake.

IV. DISCUSSION

It should be emphasized that the data do not allow preferring between the IR2 and IR3. As seen from Table 3, both runs resulted in virtually the same results. It could not be distinguished which of the fault, the dextral YŞFZ or sinistral Akçalı fault, produced the earthquake in the analysis. Both faults coincide with the nodal planes of the source mechanisms from both IR2 and IR3. Emre et al. (2005) mapped a right-lateral fault lying NW of the YŞFZ in the north of Hakkari from the field images taken from space and air. They considered this 25 km-long fault as a part of YŞFZ toward NW and assigned it a possible source of the 2005 Hakkari earthquake. Therefore, Atalay [10] had selected the NW-SE trending nodal plane resulted from the IR2 as the fault plane and proposed the earthquake faulting to be dextral. Nevertheless, in the updated active fault map of Turkey by MTA [8], this fault was drawn as thrust fault (Fig. 2), which does not coincide with the type of faulting suggested by the source mechanisms from both polarity and wave form data (Figs. 5 and 6, respectively). Therefore, we consider NE-SW trending nodal plane as the fault plane, strike of which coincides with Akçalı fault's strike. The inversion run with the NE-SW trending (strike=210°) point-source grid (e.g. the IR3) fits closely with the strike of Akçalı fault (Figs. 2, 3 and 6) and is used as a base for our discussion here.

For the IR3, the total solution requires a strike of 201°, a dip angle 69°, a rake angle of -24° and a seismic moment of 3.5×10^{17} Nm (Mw ≈ 5.7) suggesting sinistral faulting for the earthquake (Table 3; Fig. 5). The first and larger subevent with left-lateral faulting is located at a depth of 12 km just below the reference point and released a seismic moment of 3.2×10^{17} Nm in 8 s (Fig. 8) The second and smaller subevent with normal faulting dominance is located updip from the larger subevent at a depth of 6 km and 3 km NE of it. The second subevent released a seismic moment of 1.5×10^{17} Nm in 6 s that partly overlaps (about 2 s) with the rupture time of the larger subevent. We interpret these results as that the first subevent to rupture the Akçalı fault and the smaller subevent to occur along a tiny fault within the connection of the Akçalı fault with the Başkale fault zone.

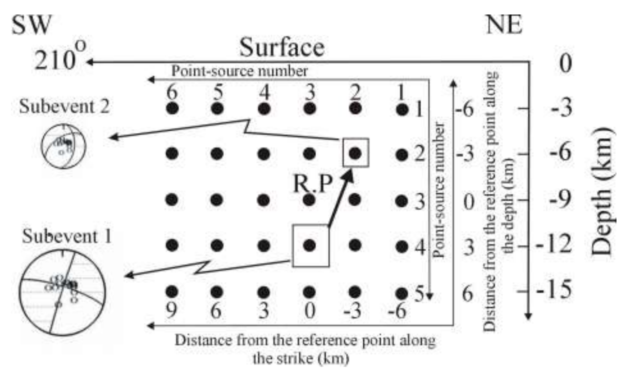

Fig. 8. Location of the subevents obtained in the inversion on the point-source grid used for the teleseismic analysis of the 25 January 2005 Hakkari earthquake. RP stands for the reference point.

The stress maps in Fig. 7 indicate that occurrence of the 2005 Hakkari earthquake increased stress along the YŞFZ and SE extend of the Akçalı fault and that stress changes over optimally oriented strike-slip faults (Fig. 7a) better explains the $M \geq 4$ seismicity after the earthquake. The fact that YŞFZ has produced main part of the following seismicity and the Fig 7a requires significant stress increase along the YŞFZ also support a rupture along the NE-SW trending fault plane and strike-slip faulting.

The occurrence of the 2005 Hakkari earthquake implicates active strike-slip faulting within the BTZ, supporting the importance of the strike-slip faulting within the eastern Anatolian block. The stressed YŞFZ seems to pose seems to earthquake hazard in the future.

V. CONCLUSIONS

The source parameters of the 25 Jaunuary 2005 Hakkari earthquake are determined from both *P* wave first motion polarities and teleseismic point-source analysis. The teleseismic *P* and *SH* waveforms are satisfactorily fitted with a double-subevent rupture model. Although which of the nodal plane represents the fault plane is not clear from the data, the local tectonic features in the epicentral area prompted us to define NE-SW trending nodal plane as the fault plane, suggesting left lateral faulting for the earthquake. The vector sum of the solution requires a strike of 201°, a dip angle 69°, a rake angle of -24° and a seismic moment of 3.5×10^{17} Nm (Mw ≈ 5.7). The first and larger subevent with left-lateral faulting and a seismic moment of 3.2×10^{17} Nm is located at a depth of 12 km while the second and smaller subevent with normal faulting dominance and a seismic moment of 1.5×10^{17} Nm is located at a depth of 6 km and 3 km NE of the larger subevent. The first subevent is interpreted to rupture the Akçalı fault while the smaller subevent to rupture a tiny fault within the connection of the Akçalı fault with the Başkale fault zone. A stress changes due to rupture along the Akçalı fault well explained the $M \geq 4$ seismicity after the earthquake, thus supporting a NE-SW striking fault. The results further suggest active strike-slip faulting within or in the very neighborhood of the Bitlis Thrust Zone.

ACKNOWLEDGMENT

This research was funded by Research Fund of the Sakarya University (Project Number: 2012-01-14-005).

REFERENCES

[1] Şengör, A. M. C., Görür, N., Şaroğlu, F., 1985 “Strike-slip faulting and related basin formation in zones of tectonic escape: Turkey as a case study, Strike-slip faulting and basin formation”, (Editors: Biddle, K. T., Christie-Blick, N.) Special Publication, Society of Economic Paleontologists and Mineralogists, 37, 227-264, 1985.

[2] Dewey, J.F., Hempton, M.R., Kidd, W. S. F, Şaroğlu, F. andŞengör, A.M.C., “Shortening of continental lithosphere: the neotectonics of Eastern Anatolia-a young collision, in Collision Tectonics”, eds. Coward, M.P. & Ries A.C., Geol. Soc. Spec. Publ., 19, pp. 3-36. B, 1986.

[3] McClusky, S., Balassanian, S., Barka, A., Demir, C., Ergintav, S., Georgiev, I., Gürkan, O., Hamburger, M., Hurst, K., Kahle, H., Kastens, K., Nadariya, M., Ouzounis, A., Paradissis, D., Peter, Y., Prilepin, M., Reilinger, R., Sanli, I., Seeger, H., Tealeb, A., Toksöz, M.N. & Veis, G., “ GPS constraints on plate kinematics and dynamics in the Eastern Mediterrenean and Caucasus”, J. geophys. Res., 105, 5695-5719, 2000.

[4] Sandvol, E., Türkelli, N. & Barazangi, M., “The Eastern Turkey Seismic Experiment: The study of a young continent-continent collision: An example from eastern Turkey”, Geophys. Res. Lett., 30(24), 8038, doi:10.1029/2003GL018912, 2003.

[5] Dhont D. and Chorowicz J “Review of the neotectonics of the Eastern Turkish–Armenian Plateau by geomorphic analysis of digital elevation model imagery”. Int J Earth Sci (Geol Rundsch) 95:34–49. doi:10.1007/s00531-005-0020-3, 2006.

[6] Reilinger, R., McClusky, S., Vernant P., Lawrence, S., Ergintav, S., Cakmak, R., Ozener, H., Kadirov, F., Guliev, I., Stepanyan, R., Nadariya, M., Hahubia, G., Mahmoud, S., Sakr, K., ArRajehi, A., Paradissis, D., Al-Aydrus, A., Prilepin, M., Guseva, T., Evren, E., Dmitrotsa, A., Filikov, SV., Gomez, F., Al-Ghazzi, R., and Karam, G. “GPS constraints on continental deformation in the Africa-Arabia-Eurasia continental collision zone and implications for the dynamics of plate interactions”, J. Geophys. Res., 111, B05411, doi:10.1029/2005JB004051, 2006.

[7] Koçyiğit, A., “2005.01.25, Mw=5.9 Sütlüce (Hakkari) Depreminin Kaynağı: Başkale Fay Kuşağı, GD Türkiye”. Deprem Sempozyumu, 23-25 Mart 2005, Kocaeli.

[8] MTA (2012). Türkiye Yenilenmiş Diri Fay Haritası, Maden Tetkik ve Arama Genel Müdürlüğü, Available: http://www.mta.gov.tr/v2.0/default.php?id=yeni_diri_fay_haritalari-goruntule.

[9] Kalafat D, Güneş Y, Kara M, Deniz P, Kekovalı K, Kuleli SH, Gülen L, Yılmazer M, Özel N “A revised and extended earthquake catalogue for Turkey since 1900(M≥4.0)”, Boğaziçi University, Kandilli Rasathanesi ve Deprem Araştırma Enstitüsü, Bebek-İstanbul, 553 pp (in Turkish), 2007.

[10] Atalay, K. “25 Ocak 2005 Hakkari Depremi (MW=5.9) Kaynak Özellikleri ve Sismotektonik Önemi”, Yüksek Lisans tezi, YYÜ Fen Bilimleri Enstitüsü, Van, 38 sf, 2007.

[11] Ambraseys NN, Finkel C, “The seismicity of Turkey and adjacent areas: a historical review, 1500-1800”, Eren Publication, İstanbul, ISBN 975-7622-38-9, 240 pp, 1995.

[12] Ambraseys N., “Earthquakes in the Mediterranean and Middle East: a multidisciplinary study of seismicity up to 1900”, Cambridge University Press. 947pp. ISBN 978-0-521-87292-8, 2009.

[13] Şengül, A., Altuncu Poyraz, S., Özvan A., Tapan M. and Kalafat D., “Hakkari-Sütlüce Depremi Fay Mekanizması Çözümleri Ve Yer-Yapı Ilişkisi Özellikleri”, İstanbul Yerbilimleri Dergisi, 23(1), 9-18 2010.

[14] Kikuchi, M., Kanamori, H., “Inversion of complex body waves-III”, Bull. Seism. Soc. Am., 81: 2335-2350, 1991.

[15] Emre,Ö., Doğan,A., Özalp, S., Yıldırım, C. “25 Ocak 2005 Hakkari Depremi Hakkında Ön Değerlendirme Raporu”, Maden Tetkik ve Arama Genel Müdürlüğü, Ankara, 2005.

[16] Toksöz MN, Nabelek J, Arpat E, “Source properties of the 1976 earthquake in eastern Turkey: a comparison of field data and teleseismic results”, Tectonophysics 49:199-205, 1978.

[17] Kalafat D., “1964-1994 yılları arasında Türkiye ve yakın çevresinde etkili olmuş depremlerin makrosismik gözlemleri. Deprem Araştırma Bülteni 73:60-97 (in Turkish), 1995.

[18] Ergin K, Güçlü U, Uz Z., “A catalogue of earthquakes for Turkey and surrounding area” İstanbul Technical University, Faculty of Mining Engineering, Earth Physics Institute, No. 24, İstanbul, 169 pp., 1967.

[19] International Seismological Centre (ISC) Available: http://www.isc.ac.uk/iscbulletin/search/bulletin/.

[20] Suetsugu D 1995 Earthquake source mechanism, IISEE Lecture note. Tsukuba, Japan

[21] Zor, E., Sandvol, E., Gürbüz, C., Türkelli, N., Seber, D., Barazangi, M., “The crustal structure of the East Anatolian plateau (Turkey) from receiver function” Geophys. Res. Lett. 30 (24): 8044, doi:10.1029/2003GL018192, 2003.

[22] Harris, R. A., “Introduction To Special Section: Stress Triggers, Stress Shadows, And Implification For Seismic Hazard”, J. Geophys. Res., 103, 24347-24358, 1998.

[23] Stein, R.S., “The Role Of Stress In The Earthquake Occurrence”, Nature, 402, 605-609, 1999.

[24] King, G. C. P, Stein, R. S., and Lin, J., “Static Stress Changes And The Triggering Of Earthquakes”, B. Seismol. Soc. Am., 84, 935-953, 1994.

[25] Okada, Y. “Internal deformation due to shear and tensile faults in a half-space”, B. Seismol. Soc. Am., 82, 1018-1040, 1992.

[26] Wells, D. L. and Coppersmith K. J. “New Empirical Relationships Among Magnitude, Rupture Length, Rupture Width, Rupture Area, and Surface Displacement”, B. Seismol. Soc. Am., 84(4), 974-1002, 1994.

First Author: is now with the Department of Geophysical Engineering, Sakarya University, 54187 Sakarya, Turkey (email: mutkucu@sakarya.edu.tr).

Third Author: is now with the Department of Geophysical Engineering, Sakarya University, 54187 Sakarya, Turkey (email: ebudakoglu@sakarya.edu.tr).

Third Author: is now with Karadeniz Technical University, Trabzon, Turkey (email: katalay@ktu.edu.tr).

Fourth Author: is now with the Department of Geological Engineering, Yüzüncü Yıl University, Van, Turkey (email: cetinyesilova@yyu.edu.tr).